

On the Relationship Between Synthesis Parameters and Morphology of the Anionic Polycaproamide Obtained in Organic Media. III. Macroporous Powders Obtained Using CO₂ and Carbodiimides as Activating Compounds

FLORIN DAN, CLEOPATRA VASILIU-OPREA

Department of Macromolecules, "Gh.Asachi" Technical University, 6600 Jassy, Romania

Received 31 January 1997; accepted 18 June 1997

ABSTRACT: The relationship between the type of activator and the morphology of polycaproamide (PCA) powders was investigated. The powders were prepared by anionic polymerization of caprolactam in ethylbenzene using sodium caprolactamate as initiator and CO₂, diisopropylcarbodiimide, and dicyclohexylcarbodiimide as activators. The powders were characterized by optical and scanning electron microscopy, particle size distribution, extent of the specific area, porosity, pore size, and pore size distribution. The crystalline structure of PCA powders was also investigated using X-ray diffraction technique. Formation of PCA powders during phase separation is discussed. Powders morphology is simultaneously and competitively controlled by the rates of polymerization and phase separation processes. It seems that the determining factor in the obtainment of such macroporous powders is the stepwise manner in which the growing centers are formed in the reaction medium. In addition, the effect of the site where polymerization proceeds after the occurrence of phase separation on the ultimate morphology of the PCA powders is also discussed. © 1998 John Wiley & Sons, Inc. *J Appl Polym Sci* **67**: 231–243, 1998

Key words: caprolactam; anionic polymerization in solvent; stepwise generation of *N*-acyllactam groups; binodal and spinodal phase separation; macroporous powders

INTRODUCTION

Low temperature anionic polymerization of caprolactam (CL) in nonpolar solvents is mainly regarded as a convenient technological process.¹ It leads to high molecular weight polycaproamide (PCA) fine suspensions, characterized by high homogeneity.² This form makes its purification easier and is very suitable for different processing procedures.^{2,3} In our previous article, the field of applicability of such particles has been briefly reviewed.⁴

The optimum polymerization conditions and physicochemical investigations on PCA chemical structure, polymolecularity, and number- and weight-average molecular weights have been reported by several authors.^{5–8} However, only a few articles were concerned with the morphology and influence of synthesis parameters on the morphology of PCA obtained in organic media.

The polymerization process is easily performed; however, phase separation and ultimate morphology are very complex and strongly related to synthesis parameters. The morphology of particles depends on the complex interaction between the polymerization and phase separation processes. Even if polymerization begins in a homogeneous medium, the solvent is a poor one for the formed

Correspondence to: C. Vasiliu-Oprea.

Journal of Applied Polymer Science, Vol. 67, 231–243 (1998)

© 1998 John Wiley & Sons, Inc.

CCC 0021-8995/98/020231-13

polymer, thus favoring polymer separation after a certain period of time. Polymer separation and its crystallization are also favored by the low reaction temperature (usually about 50–70°C below the melting point of the polymer). All the aforementioned events occur rapidly and are partly overlapped. One could expect the degree of overlapping to influence polymer morphology decisively.

The use of different catalytic systems to control the morphological development of the PCA particles presents the advantage that all of the other parameters of synthesis can be maintained at their optimal values with respect to the polymer yield and degree of polymerization. Our previous studies on the anionic polymerization of CL in organic nonpolar media clearly showed that the chemical nature of the catalytic species, especially of the activators (their efficiency), has a decisive influence on the final morphology of PCA particles.^{4,9} Thus, when aliphatic isocyanates have been used to activate the polymerization, PCA granules, resulting from the agglomeration of a large number of initially separated small particles, have been obtained. Both the size of the granules and the morphology of the individual particles composing the granules are strongly related to the type of activator, even if the activators belong to the same chemical class. The aforementioned compounds are typical activators (i.e., they react very fast, with CL yielding the *N*-acyllactam growing centers), and an induction period is not observed; the polymerization process starts with a maximum rate.

Apart from such activators, the solvent anionic polymerization of CL in the presence of carbon dioxide leads to fine PCA powders. Their extended surface was suggested by Biernacky and Wlodarczyk.² They pointed out that the anionic polymerization of CL in the presence of CO₂ in solvent is different from the typical anionic polymerization process of this monomer, because a defined amount of catalyst (e.g., *N*-acyllactam) is not introduced from the beginning into the system, and the activating species are formed stepwise in the reaction medium.

Aliphatic carbodiimides are other chemical compounds able to activate the anionic polymerization of CL and stepwise generate the growing groups.^{10,11} The common feature of all of these activating compounds is that at least two stages of initiation are required to achieve the true initiating species (i.e., *N*-acyllactams). In this case, the initiation is the rate-determining step of polymer-

ization. Specific for this process, the crystalline polymer separates from the reaction mixture, and it may be more advantageous to generate growth centers gradually, which are able to act in the liquid phase for much longer periods.

It is interesting to compare the pathway of these reactions and the morphologies of PCA particles obtained using the aforementioned activating compounds. This is because, according to our previous paper,⁹ differences in the kinetic of chemical reactions must be reflected in some changes of the ultimate morphology of PCA particles. This is why the present work is concerned with the effect of different compounds—which stepwise generates the active species (*N*-acyllactam)—on the morphology of PCA particles obtained by anionic polymerization of CL initiated with the sodium salt of CL in ethylbenzene (EB) as a reaction medium.

EXPERIMENTAL

Materials

N,N'-diisopropylcarbodiimide (DICI) and *N,N'*-dicyclohexylcarbodiimide (DCCI) were high-purity "purum" products (Fluka, Ronkonkoma, NY) and were used as received. CO₂ was dried by passing through concentrated sulfuric acid and phosphorus pentoxide deposited on glass wool. The purification of CL (technical grade, Fibrex S.A.-Savinesti, Romania) and EB (technical grade; Carom S.A.-Borzesti, Romania) have been described elsewhere.⁴

Polymerization

The PCA powders were prepared in a 100-mL, three-necked, round-bottom flask, equipped with thermometer, mechanical stirrer, and reflux condenser. The reaction flask was placed in a paraffin oil bath and the temperature was kept within $\pm 1^\circ\text{C}$. Appropriate amounts of solvent (EB) and monomer (CL) were placed into the reaction flask at 77°C and mechanically stirred. Dry nitrogen was bubbled through the solution for 5 min to exclude the air; then, a blanket of nitrogen was kept over the solution during the period of sodium caprolactamate synthesis. This one was prepared by measuring the exact amount of sodium through the extrusion of a thin cylindrical piece of metal through a calibrated glass tube. (This manner of adding sodium made it possible to reduce the ef-

fect of atmospheric moisture.) In these conditions, the reaction occurs smoothly and cleanly.² After completion of the reaction of sodium with CL, the temperature was quickly raised at 135°C, and the reaction mixture was equilibrated at this temperature.

After stopping the flow of nitrogen, a continuous stream of CO₂, used as activator for part of the experiments, was passed through the solution at a rate of 30 mL/min.

The carbodiimide activators (i.e., DICl and DCCI) were volumetrically and gravimetrically added at the reaction temperature when the aforementioned compounds were used as activators.

After 40 min, the reactions were stopped by cooling the reaction mixtures that were transferred into methanol. The PCA powder was filtered, purified by extraction in a Soxhlet with methanol, and finally dried at 50°C and 50 Pa for 24 h.

Characterization Methods

Average molecular weights were determined by viscometry using the following relation¹²:

$$[\eta] = 22.6 \times 10^{-3} \times M^{0.82}$$

Viscosity measurements were conducted in an Ubbelohde viscometer with capillary no. 1 in 85% aqueous solution of formic acid as solvent, at 25 ± 0.1°C, and at a concentration of 0.5 g/dL. Flow times were recorded as an average of three runs.

Scanning electron micrograph (SEM) photomicrographs were obtained with a JEOL JSM-840 instrument. Before examination, the powders were coated under vacuum (0.05 mbar) and under argon with a thin layer of platinum up to a depth of about 150 Å.

X-ray diffraction measurements were performed with a HZG-4A/2 diffractometer type using Ni-filtered CuK_α radiation. The scattering curves were recorded in the 8–32° interval using the step-scanning mode with a step of 0.1°.

Particle size distribution was determined with a Laser-Particle-Sizer "analysette 22" (Frisch GMBH, Idar-Oberstein, Germany), with a measuring range 0.1–527.62 μm. The powders were suspended in water and ultrasonicated 15 min before examination.

Brunauer–Emmet–Teller (BET) surface area measurements were performed in nitrogen at 77

K using a SORPTOMATIC-Carlo Erba instrument (Carlo Erba, Milano, Italy).

Mercury porosimetry was determined using an AG-65 model porosimeter (Fischer & Porter Co., Warminster, PA) able to achieve a maximum pressure of 1000 kgf/cm².

The specific surface area of wet powders, *S*, was measured by an iodine adsorption technique similar to that used by Yamaguchi and coworkers^{13,14} for determination of the specific surface area of microspheric tannin resins. The iodine adsorption method used was as follows: ~ 1 g of dry PCA powder was equilibrated in methanol and further in *n*-hexane. The PCA powder and 50 mL of 0.025 mol/L iodine in *n*-hexane were mixed with stirring for 96 h at 23°C. The residual iodine from a given volume of the supernatant solution was titrated with 0.05*N* sodium tiosulfate while stirring vigorously. The specific surface area of powders was calculated from the amount of adsorbed iodine by substituting the value of 21.1 Å² for the occupied area of the adsorbed iodine in *n*-hexane solvent.

The measurements of total pore volume, *V_p*, and porosity, *P%*, were made by using two different methods: (1) determining the apparent density of the powders, *d_a*, by the mercury pycnometric method, and the real density of polymer, *d*, measured by column-gradient method with a mixture of *n*-heptane and carbon tetrachloride; and (2) measuring the amount of solvent (*n*-hexane) that remained in the pores of the powders. For this, ~ 1 g of the powder was weighed and equilibrated in *n*-hexane as previously described. The suspended resin in *n*-hexane was heated in a water bath and filtered on a G2 glass filter at boiling solvent temperature. The increase in weight of the PCA powders allowed calculation of *V_p*. The density of *n*-hexane was determined to be 0.652 g/cm³. Porosity, *P%*, and pore volume, *V_p*, were calculated according to ref. 15:

$$P\% = (1 - d_a/d) \times 100\%$$

$$V_p = 1/d_a - 1/d$$

RESULTS

The polymerization runs performed with CO₂, DICl, and DCCI as activating compounds that gave the results listed in Table I, where the time of polymer separation (defined elsewhere; see ref. 9), *t_s*, the rate of polymerization, *V*, the high poly-

Table I Influence of Type of Activators on Anionic Polymerization of CL in EB

Activator	t_s (min)	V (%/min)	α (%)	M_w	Shape of Separated Polymer
IDI	1	12	70.5	25,500	Granules (fused aggregates)
CO ₂	3	2.2	44	15,300	Fine powders
DICI	6	1.5	55	16,800	Powders
DCCI	8	1.6	58	17,900	Powders

Reaction conditions: CL concentration, 3.0 mol/L; sodium caprolactamate concentration, 3.5 mol %/mol CL when IDI, DICI, and DCCI were used as activators; and 7.0 mol %/mol CL when CO₂ was used as activator; activator/initiator ratio, $\frac{1}{2}$ mol/mol; polymerization temperature, 135°C; polymerization time, 5 min, 30 min, and 40 min when using IDI, CO₂, and DICI or DCCI, respectively.

mer yield, the viscosimetric average molecular weight, and the aspect of the obtained polymer particles are given.

The activating effect of the investigated compounds was compared with the activity of the most widely used (by us) activator [i.e., isophorone diisocyanate (IDI)]. To obtain a systematic evaluation of their performance on this type of polymerization and the relationship between the type of activator (i.e., efficiency) and the morphology of polymer particles, all synthesis parameters were kept identical (temperature, solvent nature, initial concentration of CL, amount of catalytic species, and hydrodynamic conditions).

As shown in Table I, relatively low yields and viscometric molecular weights were obtained using these compounds. The presence in the reaction medium of a large amount of solvent requires higher concentrations of activator and initiator and favors a quicker precipitation of the formed polymer. This affects the average molecular weight (which decreases) and stops the polymerization at a low conversion. In addition, the possible polar impurities from the solvent increase the level of contamination of the whole system, thus contributing to the premature stopping of the reaction.

Using the aforementioned compounds, the time of polymer separation, t_s , is higher and the overall rate of polymerization is lower, compared with that of the polymerization conducted in the presence of IDI (Table I). For the investigated activating compounds, concomitantly with the increase of the induction period, the conversion and the corresponding average molecular weights increase too. Under the mentioned reaction conditions, the polymer is always obtained as a powder. Due to the extended surface of powders, the consistency of the reaction medium increases gradu-

ally in time, in parallel with the high polymer yield.

Particles size distributions for the PCA powders prepared by use of CO₂ and DCCI as activators are shown in Figure 1(a,b). As can be seen, both derivative curves show a unimodal size distribution pattern, but differ in shape. Thus, the differential size distribution curve of PCA-CO₂

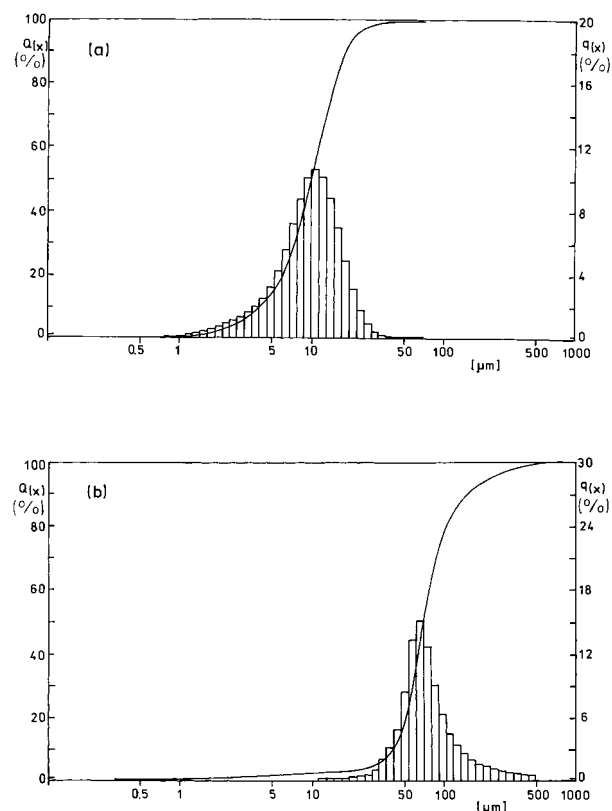


Figure 1 Particle size distribution patterns for the (a) PCA-CO₂ and (b) PCA-DCCI powders. The powders presented in all figures were prepared according to the reaction conditions given in Table I.

Table II Relationship Between the Type of Activator and the Distribution of the PCA Powder Size

Sample	
PCA-CO ₂	PCA-DCCI
Interpolation Values (0.1–500 μm)	
0.01% < 0.20 μm	0.06% < 0.20 μm
14.54% < 5 μm	1.82% < 5 μm
94.05% < 20 μm	3.48% < 20 μm
99.75% < 60 μm	32.00% < 60 μm
99.88% < 100 μm	73.88% < 100 μm
100% < 300 μm	95.58% < 300 μm
Interpolation Values (5–99%)	
5% < 5.95 μm	5% < 29.86 μm
25% < 6.69 μm	25% < 55.73 μm
40% < 8.58 μm	40% < 64.87 μm
55% < 10.43 μm	55% < 75.25 μm
75% < 13.48 μm	75% < 103.32 μm
90% < 17.68 μm	90% < 192.41 μm
99% < 24.48 μm	99% < 443.64 μm

[Fig. 1(a)] presents a long tail in the direction of lower particle size, whereas the corresponding curve of PCA-DCCI [Fig. 1(b)] has a more pronounced tail toward the higher particle size.

As shown in Table II, a narrower size distribution is obtained using CO₂ against DCCI as activator. Using the former activator, 80% of the powders have the diameter in the range of 5 to 20 μm, while using DCCI the same percentage of powder has the diameter in the range of ~ 47–280 μm.

Transmission optical micrographs of the PCA powders [Fig. 2(a–c)] show that their dimen-

sions increase concomitantly with increasing of the induction period. The finest powders are obtained when using CO₂ as activator. The PCA-CO₂ [Fig. 2(a)] and PCA-DICI [Fig. 2(b)] powders exhibit a rough (crenelated) external contour against PCA-DCCI [Fig. 2(c)] powders that display a smooth (more regular) contour.

As shown in these photos powders with intermediate sizes, but closer to those corresponding to PCA-DCCI powders, were obtained using DICI as activator. SEMs of the PCA-CO₂ [Fig. 3(a–d)] and PCA-DCCI powders [Fig. 4(a–c)] taken at different magnifications show a rough porous external structure for both investigated samples. These structures do not result from an agglomeration process, as previously observed for activators of isocyanate type.^{4,9} Thus, using CO₂ as an activating compound, the phase separation process seems to yield elongated flat “disk”-like, irregular-shaped powders, as illustrated in the low-magnification SEM photo [Figure 3(a)].

Powder shape becomes more spherical with increasing the duration of polymer separation [i.e., when DCCI was used to activate the polymerization (against CO₂)] [Fig. 4(a)]. Both the PCA-CO₂ and PCA-DCCI powders are highly porous [as shown in Fig. 3(b–d) and Fig. 4(b,c) respectively]. A more dense structure is characteristic for the PCA-CO₂ sample [Fig. 3(c)], compared with the PCA-DCCI powders [Fig. 4(c)], even if their structure is the same {i.e., a connected network type [Fig. 3(d) and Fig. 4(c)]}. In addition, the powders present large macropores on their external surface (above 1 μm) [as shown in Fig. 3(c) and Fig. 4(c)]. The network structure is a fibrillar one, with fibrils interconnected to each other. Some fibrils can also form bundles of fibrils,

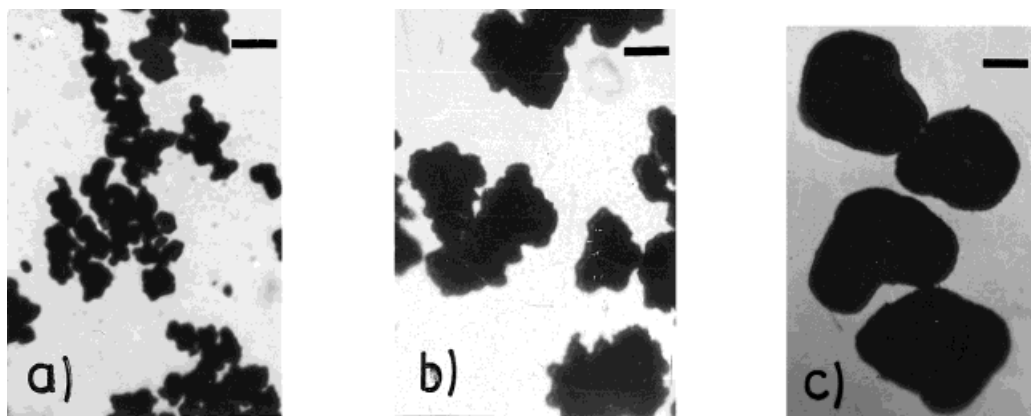


Figure 2 Optical transmission photos for the following powders: (a) PCA-CO₂; (b) PCA-DICI; and (c) PCA-DCCI. Magnification: scale bar 25 μm.

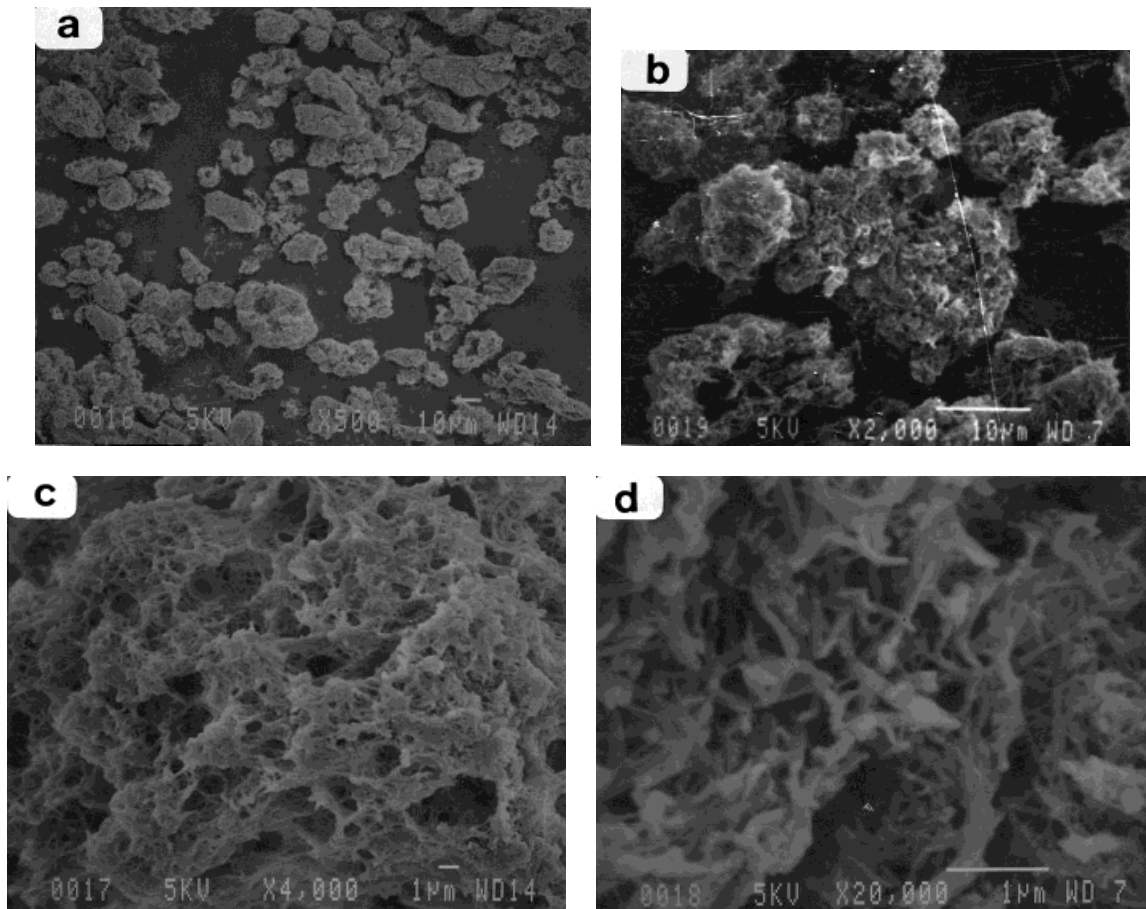


Figure 3 SEMs of the PCA-CO₂ powders at different magnifications: (a) ×200; (b) ×500; (c) ×4,000; and (d) ×20,000.

and these ones could ensure “the resistance skeleton” of the hole particle. It is evident from Fig. 3(d) and Fig. 4(c) that both the individual fibrils and bundles of fibrils can be connected to two or more similar fibrils/bundles, thus giving rise to the final network morphology.

The crystalline structure of the PCA powders was investigated using the wide-angle X-ray scattering technique. The X-ray intensity diffraction patterns for the three investigated samples are depicted in Figure 5. Clearly, all of the samples are semicrystalline polymers. They contain predominantly the α crystalline phase and a small fraction of the γ crystalline phase. However, the intensity of the peaks corresponding to the crystallographic plane α_1 (200) is stronger than those of the crystallographic plane α_2 (002, 202). Also, the half-width of the reflection peaks from the crystallographic plane α_1 (200) is lower against the corresponding ones from the plane α_2 (002,

202) (i.e., in the former crystallographic plane a more perfect crystalline lattice and higher crystals are developed¹⁶).

BET surface area measurements of the discussed powders are given in Table III. For the PCA-CO₂ powder, the obtained surface area average is 5.8 m²/g; a surface area of 3.19 m²/g was obtained for the PCA-DICI powder, and for the PCA-DCCI powder the BET value was the lowest (i.e., 1.76 m²/g). The corresponding volume of pores in the dry state are the following: 1.45 cm³/g, 1.06 cm³/g, and 0.40 cm³/g, respectively. Pore size distributions for the three investigated samples, as measured by mercury intrusion, are also given in Table III. In addition, pore volume distributions and surface distributions, as measured by mercury intrusion for the three PCA powders, are shown in Figure 6.

Several analogies, but also some differences, can be observed as concerns the pore volume

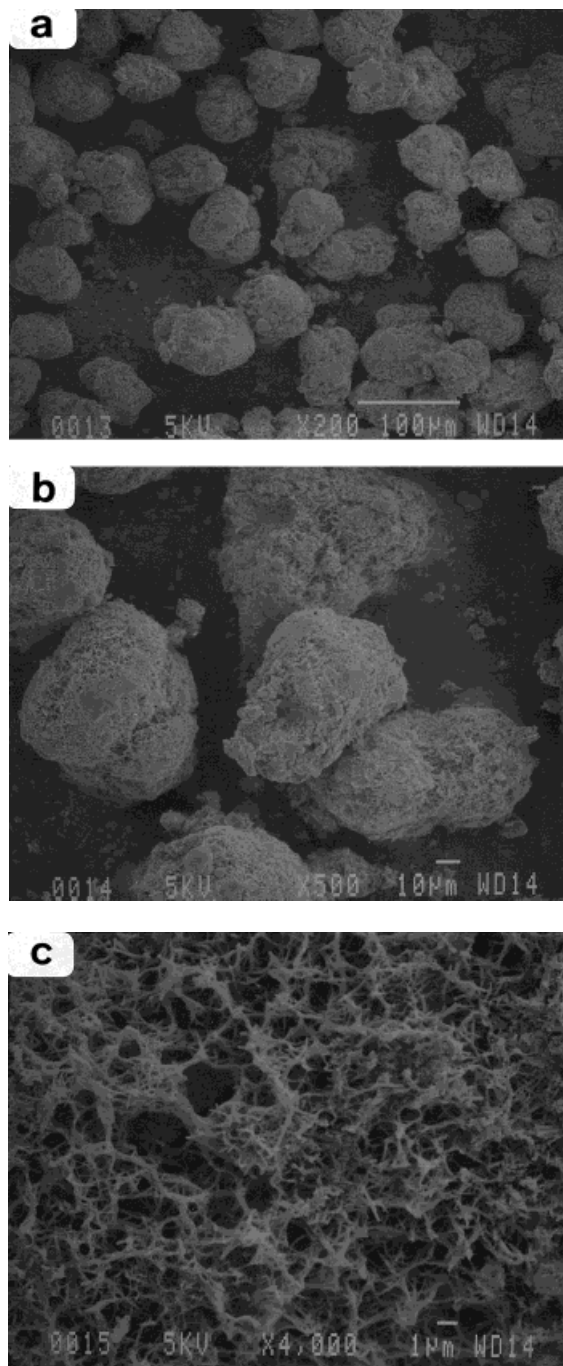


Figure 4 SEMs of the PCA-DCCI powders at different magnifications: (a) $\times 200$; (b) $\times 500$; and (c) $\times 4,000$.

distributions of the three samples (Table III and Fig. 6). Thus, PCA-CO₂ contains the lowest mesopores fraction [only 3.44% from the total pore volume (macropores, $r > 25$ nm; mesopores, $1 < r < 25$ nm; micropores, $r < 1$ nm)¹⁸], whereas PCA-DCCI contains the highest meso-

pore fraction (23.48%). The pore volume distribution of PCA-DICI is intermediate between the two aforementioned distributions. The predominant pores for both PCA-CO₂ and PCA-DICI powders correspond to the radii of 600, 1,667, and 3,000 Å, whereas for PCA-DICI and PCA-DCCI powders, the commune pores present radii of 100, 136, and 833 Å (i.e., the pore size distribution of the PCA-DICI sample resembles the distribution of PCA-DCCI powders in the region of small pores and the distribution of PCA-CO₂ powders in the region of bigger pores, respectively).

The surface distribution curves show that the smallest pores, whose contribution to the total volume of pores is small, contribute most to the extent (for all samples above 90%) of the specific surface area.

This is why the specific surface area of the wet powders was also measured by the iodine adsorption method, and the total volume of pores was measured by the liquid substitution method, using in both cases *n*-hexane as solvent. In addition, data on the total volume of pores were compared with those obtained by the mercury pycnometric method. All of the aforementioned results are collected in Table IV.

Although the liquid displacement for V_p deter-

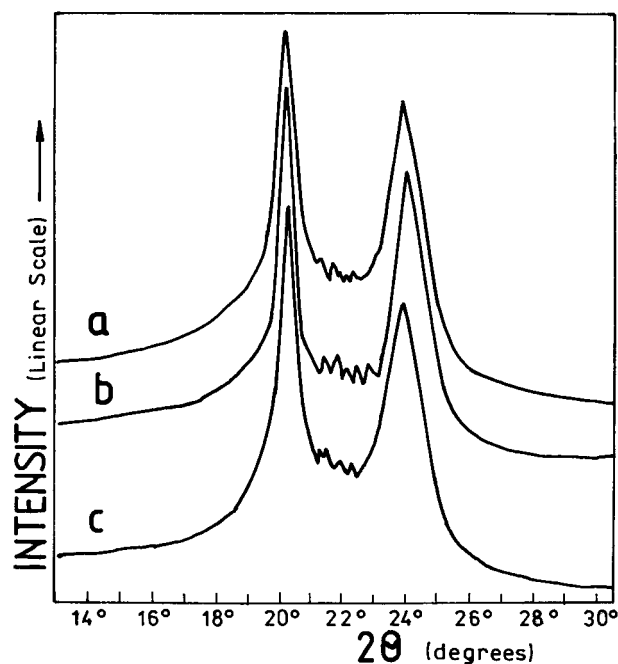


Figure 5 Typical X-ray diffraction patterns of (a) PCA-CO₂; (b) PCA-DICI; and (c) PCA-DCCI powders.

Table III Physical Properties of PCA Powders Derived from BET and Mercury Intrusion Methods

Sample	BET Area (m ² /g)	Total Pore Volume		Pore-Size Distribution ^a	
		BET (cm ³ /g)	Mercury Intrusion (cm ³ /g)	Mezopores (%)	Macropores (%)
PCA-CO ₂	5.8	1.37	1.45	3.44	96.56
PCA-DICI	3.19	0.75	1.06	8.27	91.73
PCA-DCCI	1.76	0.415	0.40	23.48	76.52

^a Macropores, $r > 25$ nm; mesopores, $1 < r < 25$ nm; and micropores, $r < 1$ nm.¹⁸

mination is only approximate, it is evident from Table IV that a good agreement exists between the total volume of pores obtained by the two different methods. Even if the differences between the values of V_p for the dry and wet powders are high, in both cases the volume of pores seems to be in the following order:

$$V_p(\text{PCA-CO}_2) > V_p(\text{PCA-DICI}) > V_p(\text{PCA-DCCI})$$

Also, PCA-CO₂ powders present the most extended surface area in both the dry and wet states. We ascribe the large differences in total surface area (the first and second columns in Tables III and IV, respectively) to the interaction between iodine molecules and polycaprolactam. It is known that iodine can very easily penetrate into the amorphous regions even in its molecular form, whereas the crystalline phase remains intact.¹⁷ Consequently, it is expected as an important fraction of iodine to be sorbed into the amorphous phases and only a small fraction to cover the external surface of PCA particles. Most likely, data obtained using the BET method reflect the real specific surface area of the investigated particles.

DISCUSSION

Based on the previously published articles^{4,9} dealing with the relation between the efficiency of aliphatic diisocyanates and the morphology of PCA granules and on the results reported herein, the following comments on the formation of PCA powders may be given.

The final morphology of the anionic PCA obtained in nonpolar solvents is achieved by a sequence of events (presented in the Introduction

section) which, under the investigated reaction conditions, occur rapidly and partly overlap. Consequently, a wide range of possible situations can be envisaged, depending on the “solubility” of the polymer and its dependence on molecular weight, and on the degree of overlapping the above events.

Crystalline morphologies described in the Results section are associated with the occurrence of some chemical and physical processes. It is well known that, in a thermally induced demixing process, the principal factors that influence the polymer morphology are liquid–liquid phase separation (i.e., thermodynamic) and vitrification (i.e., kinetic).¹⁹ Taking into account the semicrystalline structure of PCA powders, we can assume that the crystallization phenomenon occurs in a polymer-rich liquid phase, before solidification. If we regard the anionic polymerization of CL as a reaction-induced phase separation, an additional factor will strongly influence the final morphology, namely, the rate of polymerization. One can assume that the morphological development of PCA particles will be directly governed by the competition between the chemical and demixing kinetics.

Specific to the investigated process, the induction step (initiation) strongly related with the efficiency of catalytic system, is the rate-determining step of polymerization. This is why, using the same catalyst (sodium salt of CL) one of the most important factors that can influence the fine morphology is the type of activator (its chemical structure). Furthermore, not only the chemical structure of the activator but also the manner in which the growing centers are formed (i.e., instantaneously or stepwise) may influence morphology.

We suppose that the observed differences between the morphologies of PCA particles, obtained in the presence of aliphatic diisocyanates, and those corresponding to the investigated com-

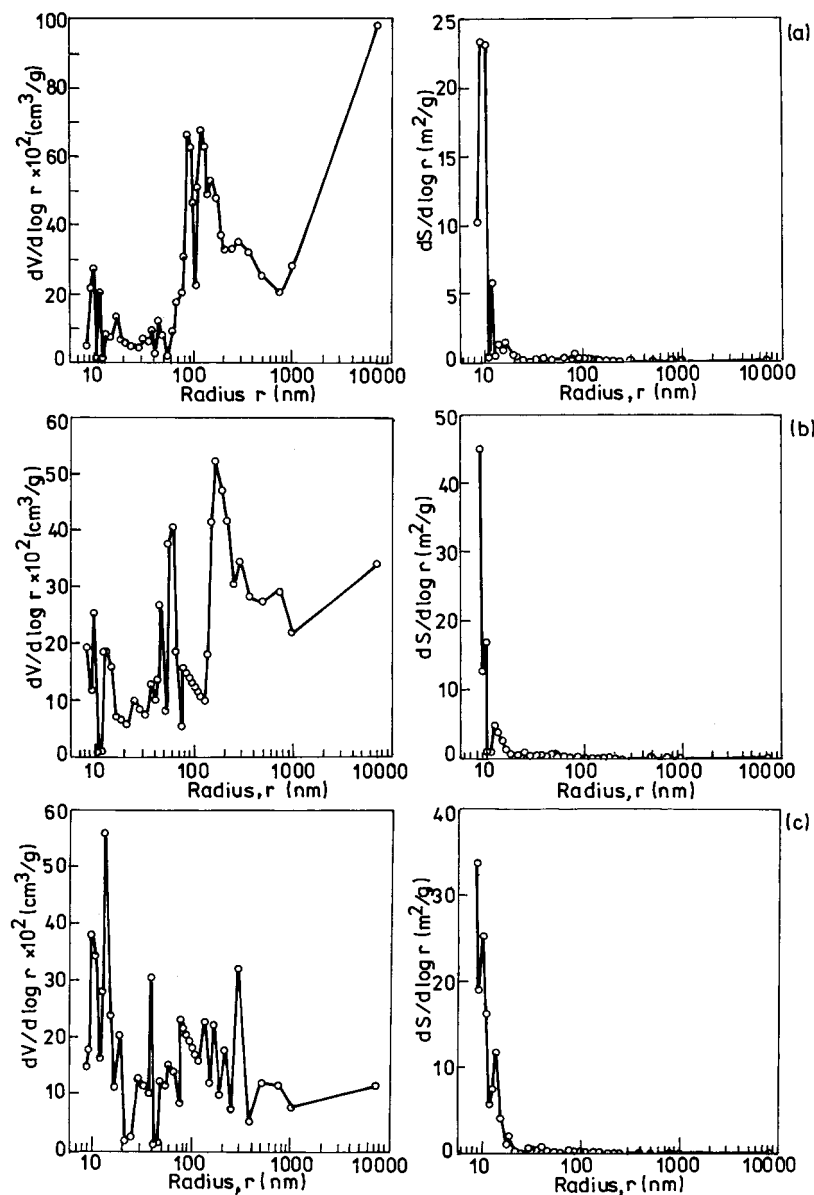
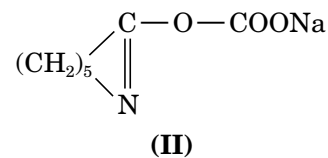
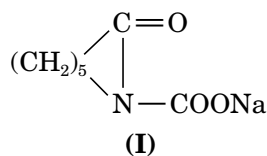


Figure 6 Mercury porosimetry-derived pore volume (left) and area distribution (right) for the following powders: (a) PCA-CO₂; (b) PCA-DICI; and (c) PCA-DCCI.

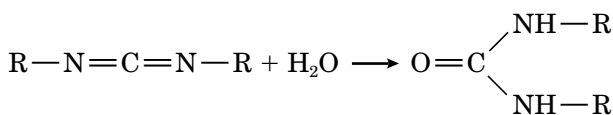
pounds, could be related to the aforementioned pathways of growing centers formation. Thus, apart from aliphatic diisocyanates, when *N*-acyl-lactam groups appear by a fast reaction of CL with isocyanates, the investigated activating compounds form stepwise the active growing centers in the reaction medium; these ones are generated as presented herein.

As a result of the reaction of the sodium salt of CL with CO₂, a mixture of *N*-(**I**) and *O*-carboxy (**II**) derivatives of CL are obtained;

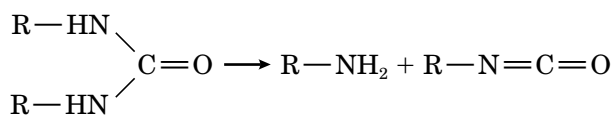


In their pioneering articles on the solvent anionic polymerization of CL in the presence of CO_2 , Chrzczonowicz and Wlodarczyk⁵ showed that the presence of the sodium salt of *O*-carboxy-caprolactim is a prerequisite for the initiation of polymerization. The period of time necessary for its formation in the system increases the induction period.

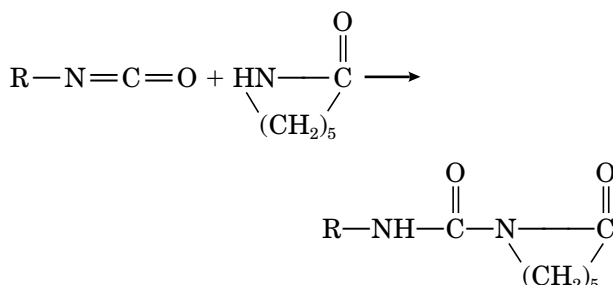
On the other hand, it has been suggested that carbodiimide compounds may react with CL in two different ways, i.e., (1) with traces of water from the reaction medium giving sym-urea



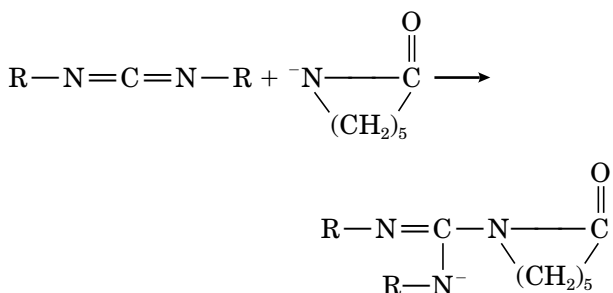
The sym-ureas further decompose to the corresponding isocyanate and amine



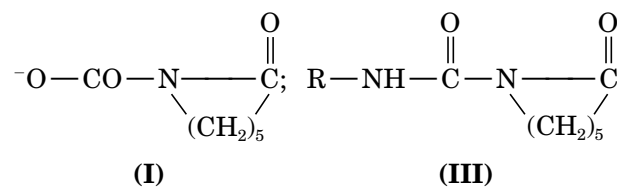
and the formed isocyanate reacts with CL giving *N*-carbamoyllactam active species



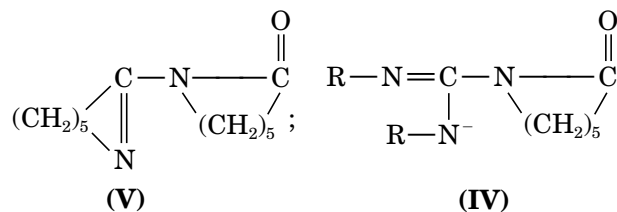
(2) Carbodiimide reacts with lactamate anion giving the compound (IV)



Consequently, two different types of structures would activate the polymerization:



or



Compound **V**, 1-(1-aza-cyclohept-1-en-2-yl)-1-azacycloheptan-2-one, could result from the reaction of CL with its *O*-carboxy derivative. We corroborated the existence of this compound with the presence of the absorption band at 881 cm^{-1} in the infrared radiation spectrum (i.e., the sodium hydrogen carbonate found by Chrzczonowicz and Wlodarczyk.⁵

Thus, the mechanisms of initiation could be the following ones: the classical activated mechanism, involving the *N*-acyllactam species **I** and **III**, or the accelerated nonactivated polymerization, involving the *N*-iminolactam derivatives²⁰ **IV** and **V**. In the first case, the found higher induction period could be also related to the inhibiting effect of amines formed in parallel with compound **III**, and/or to the acidity of compounds **I** or **II** that decrease the concentration of lactam anions in the reaction medium. However, taken into account on one hand that the anionic PCA obtained using CO_2 contains more basic terminal groups than acid ones,⁵ and on the other hand the observation that CL does not polymerize when the *O*-carboxy derivate of CL is not present in the system and our final results on the effect of the sym-ureas on the anionic CL polymerization in solvents (i.e., low yields and molecular weights), we believe that the second initiation mechanism is most probable. Specific to this, even if the induction period is not suppressed, an important accelerating effect is present.

Polymerization starts in the homogeneous medium and initially the viscosity of the reaction

Table IV Physical Properties of PCA Powders Derived from Liquid Substitution and Mercury Pycnometric Methods

Sample	Method					
	Liquid Substitution		Mercury Pycnometric			
	V_p (cm ³ /g)	S (m ² /g)	d^a (g/cm ³)	d_a (g/cm ³)	V_p^b (cm ³ /g)	P^c (%)
PCA-CO ₂	2.7	122.7	1.162	0.269	2.8	77.7
PCA-DICI	1.55	67.2	1.160	0.391	1.69	66.3
PCA-DCCI	1.44	73.9	1.159	0.435	1.45	62.6

S , specific surface area; V_p , total pore volume; $P\%$, porosity.

^a Measured by the density-gradient method with *n*-hexane and carbon tetrachloride.

^b Evaluated by equation: $V_p = 1/d_0 - 1/d$.

^c Evaluated by equation: $P\% = 1 - d_0/d \times 100\%$.

mixture slightly increases, mainly due to the formation of salts of some of the products.²¹ In the meantime, the number of stepwise-generated active centers (i.e., *N*-acyllactam groups) becomes significant, in order that the growing of chains to occurs, and a faint opalescence appears, thus indicating the occurrence of a phase separation. The solution itself demixes into a polymer-rich and a “solvent”-rich phase, but the connectivity of the polymer-rich phase is rapidly interrupted under the intervention of the shear gradient and by an increase of the interfacial tension, resulting in a droplet-type morphology. In this stage, one can assume that each droplet has the consistency of a viscous semiliquid medium. Considering now, the droplet itself as an isolated system, the phase separation will proceed within each droplet. If the droplet has a such composition (i.e., polymer, monomer, and “solvent”) that a slight increase of polymer concentration (due to the chemical reaction) is able to induce a spinodal decomposition, bicontinuous structures of both segregate phases are obtained [Fig. 3(c,d) and Fig. 4(c)]. Because the reaction temperature is well below (~ 50 – 70°C) the melting point of the polymer, the polymer-rich phase will solidify, with the phase separation process being stopped. The solidified polymer forms a continuous structure giving the powder physical cohesion, whereas the solvent that fills the empty spaces forms, together with the reaction medium, a continuous liquid phase in which solid particles are suspended.

Another possible mechanism of phase separation could be “the spinodal nucleation” mechanism suggested by Binder,²² wherein the gradual transition from nucleation to spinodal decomposi-

tion occurs. This mechanism supposes that phase separation starts by the formation of diffuse ramified clusters, but these ones first have to compact and then grow. Tacking into account the shape of the smaller particles from SEM photos, Figure 3(b) and Figure 4(b), we believe that this mechanism is not specific for the anionic polymerization of CL in the presence of the investigated activating compounds.

On the other hand, phase separation could take place either by formation and growth from the outset of phase separation of the polymer-rich droplets or by an alternate mechanism, this implying a continuous separation of polymer-rich droplets and growth with a coalescence of different-sized segregated particles into final powders. As observed, for the investigated activating compounds, the period of time required by phase separation is obviously short, so that most likely phase separation does not occur continuously, except during the beginning stages of the process. This assumption is in agreement with the particle “inhibiting region”²³ concept, which considers that the surrounding area of the particle disturbs the appearance and the existence of other microparticles. In this case, lowering of the surface energy through the growth of the existing particles is thermodynamically favored over formation of new particles.

Subsequently, there are three possible polymerization sites, namely in the homogeneous phase, inside of the particle, and at the surface of large particles. Overall, polymerization is expected to proceed predominantly inside and at the surface of the large particles; however, this does not mean that polymerization reactions occurring

in the homogeneous phase are negligible. These assumptions are in agreement with the low monomer concentration in the reaction medium, the high porosity, and extended surface of the powders, and with the high affinity between the already separated polymer, monomer, and catalytic species.

Figure 3(a,b) and Figure 4(a,b) show two frequently observed deviations from the general shape of the powders (i.e., asymmetric powders and small particles can be identified). It is likely that a fraction of oligomeric chains soluble in the reaction medium is adsorbed into porous particles or on the surface of separated particles. As a consequence of the polymerization, inside the particles the total volume of pores decreases and the specific surface area of the powder increases. When the soluble growing chains are adsorbed and situated on particle surface, the subsequent polymerization may lead to asymmetric powders. Occasionally, double or even triple particles can be observed, especially in the case of PCA-DCCI powders [Fig. 4(a,b)], these ones may result from coalescence when one particle is already solidified and another just segregates.

The competition between powders growth by the absorption of catalytic species, as well as of soluble growing chains onto preexisting particles, and the formation of new particles in the homogeneous medium, also allows the formation of observed small particles. This behavior is characteristic for the later stages of polymerization when the reaction medium contains a low monomer concentration and is a poorer solvent for the formed polymer.

CONCLUSIONS

Macroporous PCA powders may be prepared by anionic polymerization of CL in nonpolar aromatic solvents in the presence of the sodium salt of CL as initiator and CO₂ or aliphatic carbodiimides as activating compounds.

The genesis of these powders may be explained by taking into account the possibility of liquid-liquid phase separation induced by the polymerization reaction and subsequently the polymer crystallization in a confined space.

Specific to the investigated activating compounds, the stepwise manner in which the growing centers are formed is able to induce a spinodal decomposition within the already separated polymer-rich droplets.

Thus, the prepared PCA powders present a network-type internal structure (interconnected fibrils), a high porosity, and an extended specific area; their crystalline structure contains almost the entire α crystalline phase.

The shape of powders, their size distributions, and fine morphology (i.e., total volume of pores, pore size, pore size distribution, and the extent of specific area) are influenced both by the relative efficiency of the activators and by the "competition" between the sites where polymerization proceeds (after the demixing process has occurred).

The authors are grateful to Professor G. Riess, (the École Nationale Supérieure de Chimie de Mulhouse, France) for supplying the carbodiimide derivatives used in this study. Thanks are due to Dr. F. Mertz for his assistance in performing the SEMs. Special acknowledgments are made to Mr. M. Hübner, Deputy Director, and to Mr. U. Gerber, Head of the Application Laboratory of Fritsch GMBH Manufacturers of Laboratory Instruments (Idar-Oberstein, Germany), for the courtesy of performing the size distribution measurements of the PCA powders. The authors are also indebted to Mrs. B. Gugu and Miss M. Iordache (CAROM S.A.-Borzești, Romania) for performing the BET and mercury intrusion measurements.

REFERENCES

1. S. Chrzczonowicz, M. Włodarczyk, and O. Ostaszewski, *Makromol. Chem.*, **38**, 159 (1960).
2. P. Biernacki and M. Włodarczyk, *Eur. Polym. J.*, **16**, 843 (1980).
3. A. Sahler, Brit. Patent, 1,118,700 (1969), *Chem. Abstr.*, **69**, 44633 (1968).
4. Cl. Vasiliu-Oprea and F. Dan, *J. Appl. Polym. Sci.*, **62**, 1517 (1996).
5. S. Chrzczonowicz and M. Włodarczyk, *Makromol. Chem.*, **48**, 135 (1961).
6. V. Kubanek, J. Kralicek, and A. Moucha, *Scientific Papers of the Prague Instit. Chem. Technol.*, **C24**, 9 (1976).
7. P. Biernacki, S. Chrzczonowicz, and M. Włodarczyk, *Eur. Polym. J.*, **7**, 739 (1971).
8. P. Biernacki and M. Włodarczyk, *Eur. Polym. J.*, **11**, 107 (1975).
9. Cl. Vasiliu-Oprea and F. Dan, *J. Appl. Polym. Sci.*, **64**, 2575 (1997).
10. J. Stehlicek, J. Sebenda, and O. Wichterle, *Collect. Czech. Chem. Commun.*, **29**, 1236 (1964).
11. G. Stea and G. B. Gechele, *Eur. Polym. J.*, **6**, 233 (1970).
12. J. Brandurp and E. H. Immergut, Eds., *Polymer Handbook*, John Wiley & Sons, Inc., New York, 1975.

13. H. Yamaguchi, M. Higuchi, and I. Sakata, *J. Appl. Polym. Sci.*, **45**, 1455 (1992).
14. H. Yamaguchi, R. Higashida, M. Higuchi, and I. Sakata, *J. Appl. Polym. Sci.*, **45**, 1463 (1992).
15. O. Okay and C. Gurun, *J. Appl. Polym. Sci.*, **46**, 401 (1992).
16. H. M. Heuevel, R. Huisman, and K. C. J. B. Lind, *J. Polym. Sci.*, **14**, 921 (1976).
17. J. Baldrian, *Collect. Czech. Chem. Commun.*, **31**, 1017 (1966).
18. K. M. Daer and Y. A. Levendis, *J. Appl. Polym. Sci.*, **45**, 2061 (1992).
19. A. Keller, *Macromol. Symp.*, **98**, 1 (1995).
20. J. Brozek, M. Marek, J. Roda, and J. Kralicek, *Macromol. Chem.*, **189**, 17 (1988).
21. J. Stehlicek and J. Sebenda, *Eur. Polym. J.*, **22**, 769 (1986).
22. K. Binder, *Adv. Polym. Sci.*, **112**, 181 (1994).
23. Y. Naka and Y. Yamamoto, *J. Polym. Sci. Polym. Chem. Ed.*, **30**, 1287 (1992).